PETRA Sequence for Catheter Detection in Interstitial High-Dose-Rate (HDR) Brachytherapy

Evangelia Kaza, Ph.D.; Ivan Buzurovic, Ph.D.

Brigham and Women's Hospital, Dana-Farber Cancer Institute, Harvard Medical School, Boston, MA, USA

Introduction

In high-dose-rate (HDR) interstitial brachytherapy treatment planning, determining the dwell positions of radioactive sources relies on accurate localization of the implanted catheters. Currently, catheters are detected in-situ using CT, followed by T2-weighted MRI for target and organs at risk (OARs) delineation. Possible changes in organ or catheter position between the two scans can lead to registration errors in the MR-CT image fusion and affect estimated dose [1]. Brachytherapy dose calculations are performed assuming water as the medium [2], unlike external beam radiotherapy applications which require tissue-related Hounsfield units obtained from CT. Therefore, brachytherapy treatment planning could be performed using MRI only, if it could detect brachytherapy devices with acceptable spatial accuracy. However, brachytherapy applicators, templates, and catheters present no signal on standard MR images, and are thus difficult to discern from surrounding air, vessels, or low signal intensity tissues. Approaches to visualize interstitial catheters include insertion of markers [3] which incur additional costs, or investigational post-processing software to take advantage of magnetic susceptibility differences between metal or air and tissues [4].

Our goal was to detect empty interstitial needles and templates for HDR brachytherapy directly on clinical MR images obtained on a 3T MAGNETOM Vida scanner (Siemens Healthcare, Erlangen, Germany) used for radiotherapy simulations. An FDA approved "pointwise encoding time reduction with radial acquisition" (PETRA) sequence was selected and optimized for this purpose. As a zero TE (ZTE) sequence variant able to image tissues with T2 < 1 ms [5], PETRA was promising for visualizing synthetic polymers whose transverse relaxation times in the order of µs–ms cannot be captured by the longer echo times employed by most clinical sequences. PETRA can provide submillimetre isotropic resolution and is robust to motion artifacts owing to its mainly radial acquisition scheme. Moreover, its 3D properties allow for accurate reconstruction in all 3 orientations, which is important for treatment planning.

Methods

Phantom

Detectability of empty interstitial needles on PETRA images and their positional agreement with CT was investigated using a poultry phantom. A plastic obturator attached to a Syed-Neblett interstitial template (Best Medical International, Springfield, VA, USA) with six ProGuide Sharp Needles 6Fx294mm (Elekta Brachytherapy, Stockholm, Sweden) in the obturator slots was introduced into the giblet filled cavity of a cleaned turkey. Three additional needles were inserted in the turkey breast through the template. The poultry phantom with empty catheters was scanned in the 3T MAGNETOM Vida using a coronal 3D PETRA (TR/TE 3.32/0.07 ms; FOV 300 mm^3 isotropic; voxel size 0.85 mm^3 isotropic; flip angle 6°; bandwidth 400 Hz/px; 100000 radial views; acquisition time 5 min 46 s), and subsequently CT imaged. PETRA MR and CT images were fused by applying a rigid body registration. The coordinates of interstitial catheters on the CT and on the co-registered MR images were extracted for each slice location, and their Euclidean distance was calculated. The mean, median and standard deviation of this metric over all slices were computed as global measures of MR-CT distance for each catheter.

Patients

The feasibility of PETRA's clinical implementation for interstitial needle and template detection was assessed on five gynaecological brachytherapy patients. Anesthetized patients were implanted under ultrasound guidance with a Syed-Neblett interstitial template and ProGuide Sharp Needles in the HDR suite. The catheters were filled with copper strands and patients were imaged on a helical CT.

After marker removal, patients were transferred on a BioMatrix Dockable Table and transported to the MR suite, where they were scanned using a bottom BioMatrix Spine 32 coil and a top Body 18 Long coil. Axial T2-weighted 3D SPACE images (TR/TE 1800/167 ms; FOV 288 × 288; voxel size 1.04 mm^3 isotropic; flip angle 120°; bandwidth 668 Hz/px; acquisition time 11 min 11 s) were acquired for lesion and OAR contouring. Axial 3D PETRA images

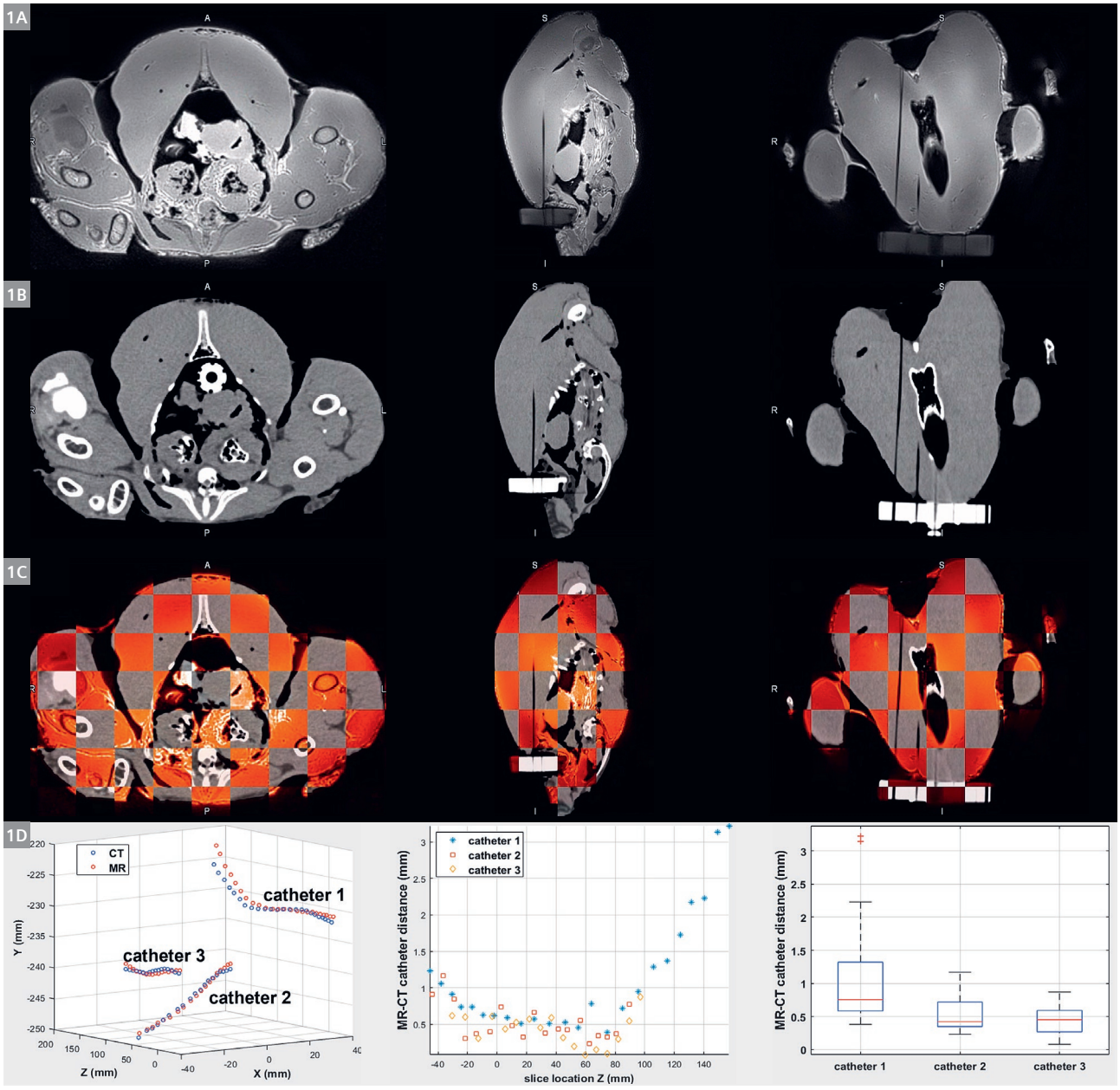

1 **(1A)** PETRA, **(1B)** CT images of a poultry phantom in axial, sagittal, and coronal orientation. Three empty plastic catheters penetrating the turkey breast through an interstitial template were detected with negative contrast. **(1C)** Checkerboard view of the PETRA (red) and CT images (grey) fusion in the three planes. **(1D)** Left: 3D plot of the CT (blue) and PETRA MR (red) coordinates of the points used to track the three interstitial catheters. X: right-left, Y: anterior-posterior, Z: superior-inferior axis. Catheter numbers increased from left to right on the phantom images. Middle: distance between CT and MR point contour coordinates over their common slice locations Z for each catheter. Right: Boxplots of MR-CT point distances for each catheter. Red lines: median; whiskers: minimum and maximum measurement; red crosses: outliers. *Reprinted with permission from [7].*

(TR/TE 3.32/0.07 ms; FOV 416 mm³ isotropic; voxel size 0.90 mm³ isotropic; flip angle 4°; bandwidth 401 Hz/px; 100000 radial views; acquisition time 5 min 55 s) were acquired to investigate needle detectability. Feasibility assessments of tracking empty interstitial catheters on PETRA images and of producing treatment plans using the MR scans only were performed in a treatment planning system (TPS).

Results

Phantom

PETRA detected the empty interstitial needles with negative contrast and the template with intermediate contrast relative to the turkey tissue (Fig. 1A). The plastic obturator and catheter sections outside the poultry flesh were not visualized. PETRA-CT fusion showed very good positional agreement of turkey features and interstitial catheters between the two modalities (Fig. 1C). For all three catheters, the distance of their tracked points on PETRA and CT images was < 1 mm for slice locations between -30 and 100 mm (Fig. 1D). The leftmost catheter 1 with a longer interstitial section presented increasing MR-CT catheter distance for slice locations > 100 mm. Median MR-CT catheter distance was < 1 mm for all catheters, while average distance amounted to 1.12 ± 0.81 mm (mean ± standard deviation) for catheter 1 due to increasing divergence of PETRA and CT catheter positions for slices further from isocenter.

Patients

Figure 2 shows matching CT and MR slices of an example patient. Using PETRA, all empty interstitial catheters could be identified with opposite signal than the marker-filled catheters on CT. In general, catheter locations agreed between MR and CT, considering slight variations in patient position between the two examinations. Nevertheless, organ and needle positions matched better between the

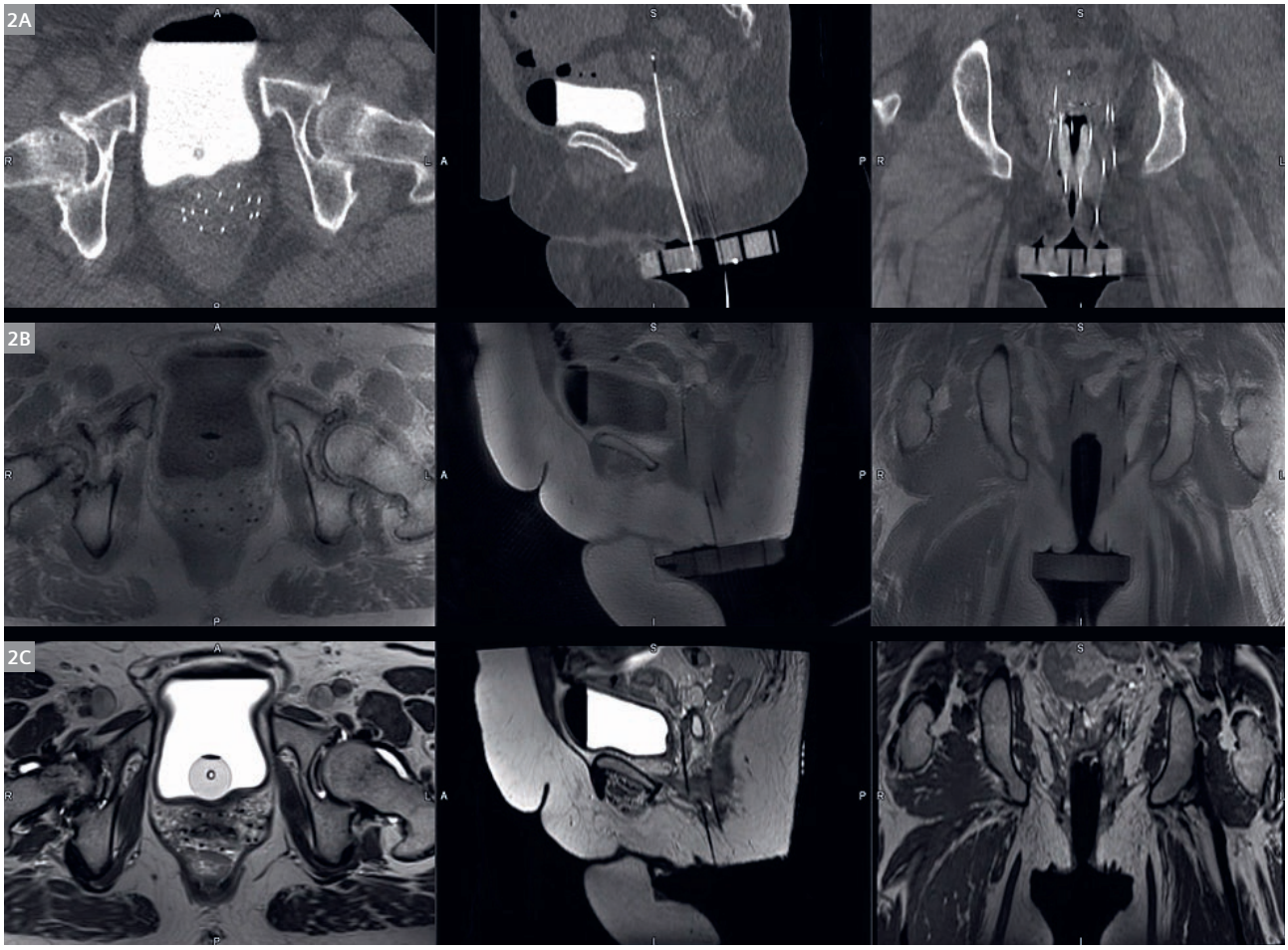

2 Axial (left), sagittal (middle) and coronal (right) images of an endometrial adenocarcinoma patient with 14 interstitial needles perforating a Syed-Neblett template. **(2A)** CT, with copper-filled catheters appearing bright. **(2B)** PETRA with empty catheters detectable by their lack of signal inside tissue, and visible template. **(2C)** SPACE with obscured template, and dark empty catheters more ambiguously differentiated from low signal intensity tissues.

MR datasets which were acquired immediately after each other in the same session. While catheters appeared hypointense on both PETRA and SPACE images, PETRA provided higher spatial resolution and a lower range of overall image contrast than SPACE, which facilitated catheter differentiation from surrounding tissues. The obturator was not visualized on either MR scan, but the interstitial template was well distinguished from the background air on PETRA, contrary to SPACE. Thanks to template visualization on PETRA, interstitial catheters could be followed to their entry hole on the template, allowing for individual catheter identification (Fig. 3A). All empty needles could be tracked on PETRA images using a TPS. Treatment plans could be produced by combining catheter tracking information from PETRA with organ and lesion contours obtained from SPACE (Fig. 3B).

Discussion

Initial PETRA images of a poultry phantom revealed the potential to detect empty interstitial needles with negative contrast, and a clinically acceptable [6] sub-millimetre accuracy compared to CT within 10 cm from scanner isocenter. Increasing disagreement with distance from isocenter may be due to geometric distortions caused by residual gradient non-linearities [7] or to registration errors during fusion. Utilization of a phantom for assessing spatial agreement of PETRA and CT eliminated uncertainties introduced by possible patient position mismatch in clinical scenarios.

Observations for interstitial template and catheter visualization on PETRA images of gynaecological brachytherapy patients were similar as for the phantom. The minimal echo time allowed capturing MR signal from the plastic template but not from the obturator which is made from a different material. The employed low flip angle resulted in a short range of tissue intensities, providing more consistent tissue-catheter contrast than the T2-weighted SPACE, where parts of the lesion also appeared hypointense. This fact, combined with PETRA's high spatial resolution and lower susceptibility-induced distortions than T2-weighted imaging [7] made catheter detection more accurate on PETRA than on SPACE. The additional advantage of determining catheter entry holes on the template allowed for catheter identification. Since a TPS could trace all catheters on PETRA, treatment plans could be produced by fusing SPACE images for treatment contour delineation with the spatially matching PETRA images for needle detection. These plans were comparable to those obtained using the standard CT-based catheter tracking [7], presenting PETRA's potential to replace CT for this purpose. MR-only brachytherapy treatment planning would avoid MR-CT misregistration, reduce anaesthesia time for patients undergoing intra-operative imaging, and spare hospital resources.

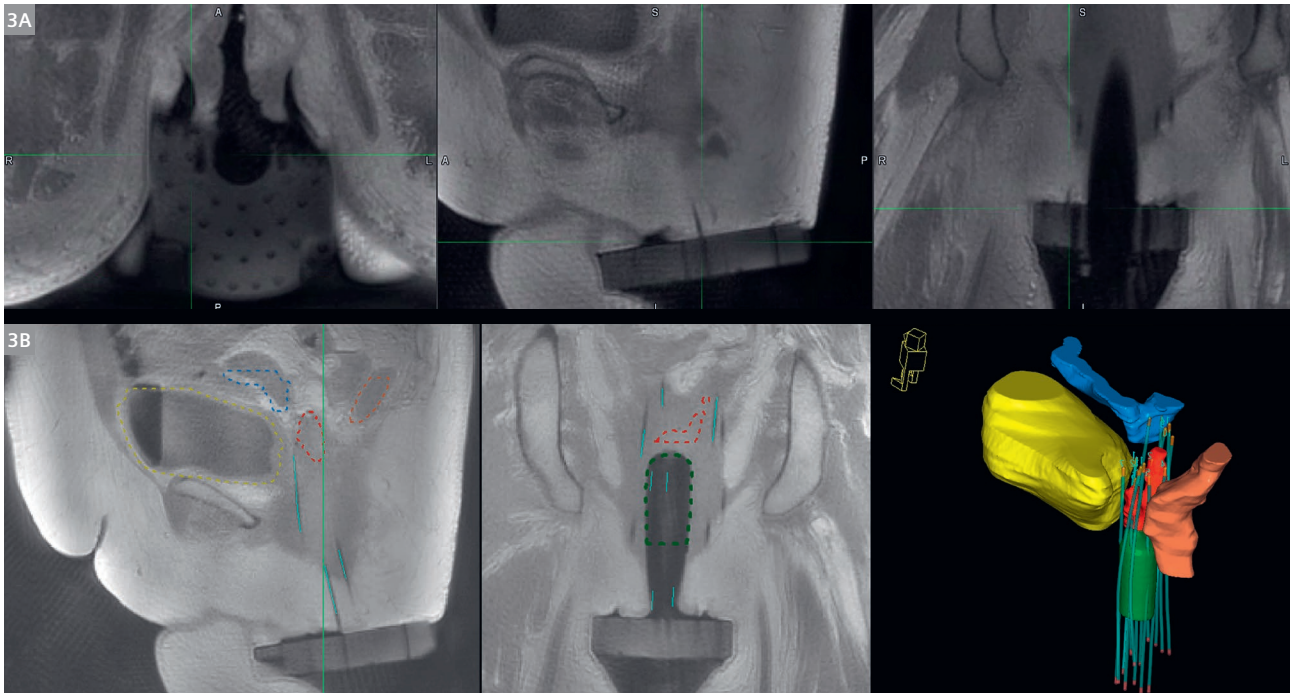

3 **(3A)** PETRA images of an endometrial adenocarcinoma patient zoomed on the interstitial template in all three orientations, with green crosshairs indicating the entry hole of a tracked catheter. **(3B)** Left, middle: sagittal and coronal PETRA views, with overlapping dotted lines indicating contoured structures and turquoise lines showing catheters tracked in a TPS. Right: 3D reconstruction of tracked catheters (turquoise), obturator (green), tumor (red), bladder (yellow), rectum (orange), and bowel (blue). *Reprinted with permission from [7].*

Conclusion

Interstitial HDR brachytherapy catheters and templates were detected on PETRA images of a poultry phantom and of gynaecological cancer patients. Catheters were traceable in a TPS, providing adequate information for treatment plan production. PETRA implementation may pave the way to MR-only treatment planning in interstitial HDR brachytherapy.

Contact

Evangelia Kaza, Ph.D.
Instructor in Radiation Oncology
Brigham and Women's Hospital
Department of Radiation Oncology
75 Francis Street
Boston, MA, 02115
USA
Ekaza1@bwh.harvard.edu

Ivan Buzurovic, Ph.D.
Assistant Professor of Radiation Oncology
Brigham and Women's Hospital
Department of Radiation Oncology
75 Francis Street
Boston, MA, 02115
USA
Ibuzurovic@bwh.harvard

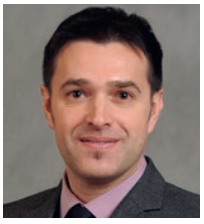

References

1 Kirisits C, Rivard MJ, Baltas D, Ballester F, De Brabandere M, Van Der Laarse R, et al. Review of clinical brachytherapy uncertainties: Analysis guidelines of GEC-ESTRO and the AAPM. Radiother Oncol. 2014;110(1):199–212.
2 Sander T. Air kerma and absorbed dose standards for reference dosimetry in brachytherapy. Br J Radiol. 2014;87(1041).
3 Ning MS, Vedam S, Ma J, Stafford RJ, Bruno TL, Cunningham M, et al. Clinical utility and value contribution of an MRI-positive line marker for image-guided brachytherapy in gynecologic malignancies. Brachytherapy. 2020;19(3):305–15.
4 Nosrati R, Paudel M, Ravi A, Pejovic-Milic A, Morton G, Stanisz GJ. Potential applications of the quantitative susceptibility mapping (QSM) in MR-guided radiation therapy. Phys Med Biol [Internet]. 2019;64(14):ab2623. Available from: https://doi.org/10.1088/1361-6560/ab2623
5 Grodzki DM, Jakob PM, Heismann B. Ultrashort echo time imaging using pointwise encoding time reduction with radial acquisition (PETRA). Magn Reson Med. 2012;67(2):510–8.
6 Nath R, Anderson LL, Meli JA, Olch AJ, Stitt JA, Williamson JF. Code of practice for brachytherapy physics: Report of the AAPM radiation therapy committee task group no. 56. Med Phys. 1997;24(10):1557–98.
7 Kaza E, Lee CY, King MT, Dyer MA, Cormack RA, Buzurovic I. cFirst pointwise encoding time reduction with radial acquisition (PETRA) implementation for catheter detection in interstitial high-dose-rate (HDR) brachytherapy. Brachytherapy 2022, in press.